



Continuous new particle formation in a Mediterranean coastal environment: Insights from atmospheric ions behaviour analysis

Nikos Kalivitis¹, Spyridon-Emmanouil Markoulakis¹, Panayiotis Kalkavouras², Veli-Matti
5 Kerminen³, Markku T. Kulmala³ and Maria Kanakidou^{1,4,5}

¹ Environmental Chemical Processes Laboratory (ECPL), Department of Chemistry, University of Crete, 70013, Heraklion, Greece

² School of Natural Sciences, Physics, Centre for Climate & Air Pollution Studies (C-CAPS), Ryan Institute, University of Galway, H91 CF50, Galway, Ireland

10 ³ Institute for Atmospheric and Earth System Research / Physics, Faculty of Science, University of Helsinki, 00014, Helsinki, Finland

⁴ Center for the Study of Air Quality and Climate Change (C-STACC), Institute of Chemical Engineering Sciences (ICE-HT), Foundation for Research and Technology, Hellas (FORTH), Patras, Greece

15 ⁵ Laboratory for Modelling and Observation of the Earth System (LAMOS), Institute of Environmental Physics (IUP), University of Bremen, Bremen, Germany

Correspondence to: Nikos Kalivitis (nkalivitis@uoc.gr)

Abstract. Atmospheric new particle formation (NPF) is crucial for aerosol number concentration and for studying the production processes of secondary aerosol particles. NPF events are commonly classified based on visible particle growth, and their occurrence frequency is often underestimated. Recent methodologies propose that “quiet” NPF (QNPF) events, which are not traditionally classified as NPF events, can contribute significantly to particle number concentrations. This study presents three-years (June 2020 - May 2023) of observations of ion and particle size distributions performed at the Finokalia environmental research station in Crete, Greece, using a Neutral cluster and Air Ion Spectrometer (NAIS) and a Mobility Particle Size Spectrometer (MPSS). By analysing the observed ion number size distributions and applying a nanoparticle ranking analysis method, this study reveals that QNPF events are frequent and contribute significantly to particle formation and growth in the Eastern Mediterranean. Negatively charged intermediate size ions are found to be reliable indicators of particle formation, including both classical NPF and QNPF episodes. Our analysis indicates continuous particle formation even on days traditionally classified as “non-event” days, providing fundamentally new understanding of NPF processes in the region.



30 1 Introduction

New particle formation (NPF) is a complex process consisting of the production of low-volatility vapours, clustering of those vapours, atmospheric nucleation, cluster's stabilization, activation of the clusters with afresh vapours, and gradually growth towards larger sizes via condensation (Kulmala et al., 2014). NPF is considered to be the major source of aerosol numbers to the terrestrial atmosphere (Zhang et al., 2012), while a large fraction of CCN in the global atmosphere may originate from these processes (Merikanto et al., 2009).

NPF events are observed worldwide, from boreal forests to megacities and all year round (Nieminen et al., 2018). However, particle number concentrations (PNC) from NPF at a specific location, are highly dependent on the prevailing environmental and meteorological conditions. Usually, reduced amount of particle pollution, thus low condensation sink (CS) and sufficient precursor vapours, such as sulfuric acid (H_2SO_4), ammonia (NH_3), amines, volatile organic compounds (VOCs) and iodine under high temperatures, low relative humidity and intense solar radiation promote NPF (Kerminen et al., 2018; Wang et al., 2022). NPF episodes were also identified under high number of pre-existing particles (Kulmala et al., 2017; Yan et al., 2021) and also occurred during the night or started during the day and continued throughout the following night (Kalivitis et al., 2012; 2019).

In the Eastern Mediterranean coastal environment, regional NPF has been observed to take place frequently (Kalivitis et al., 2008; Pikridas et al., 2012; Kopanakis et al., 2013; Kalivitis et al., 2019; Kalkavouras et al., 2021; Baalbaki et al., 2021; Aktypis et al., 2024). In the island of Crete, Greece, an annual frequency of 27% (undefined days were 23%) has been found, using 10 years of particle number size distribution (PNSD) measurements, being less frequent than in other European locations (Kalivitis et al., 2019).

To identify NPF events and characterize their dynamics, event-based methods have been utilized by visually inspecting PNSD and classifying days according to whether formation and subsequent growth can be observed (Dal Maso et al., 2005; Kulmala et al., 2012). However, such an approach has certain limitations, as several days may not be classified in an unambiguous manner and are therefore characterized as “undefined”, since they do not fulfil the criteria of an event day, although some indication of particle formation is apparent (Buenrostro Mazon et al., 2009). Furthermore, the calculation of the growth rate (GR) of newly formed particles is only possible on days when a distinct nucleation-mode (particles with diameters below 25 nm) appears in the size distribution, and can grow undisturbed and without air mass changes for several hours (Dal Maso et al., 2005; Kulmala et al., 2012). This limitation introduces significant uncertainty in GR seasonality, range and variability, as the analysis is inevitably restricted to a small number of events per location per year.

Atmospheric ion observations may be used to more robustly identify and characterize NPF. Atmospheric ions can be classified by size into i) small (<1.6 nm), ii) intermediate (1.6-7.4 nm) and iii) large ions (>7.4 nm) (Hirsikko et al., 2011). Small ions are continuously generated in the atmosphere through ionisation processes. In the lower atmosphere, these ions primarily originate from natural radioactivity, particularly the radioactive decay of radon (^{222}Rn), a gas which diffuses into the atmosphere from the soil (Chen et al., 2016). The presence of radon and its decay products have a significant impact on ion concentrations in the atmospheric surface layer, particularly over land (Komppula et al., 2007). By contrast, in the upper



65 troposphere and lower stratosphere, galactic cosmic rays (GCRs) are the main source of ionization. GCRs ionise air molecules through high-energy collisions, which makes them really important in regions with low surface emissions, such as over oceans and in polar areas (Zhang et al., 2011). Large ions are generally formed when small ions attach to pre-existing aerosol particles. Intermediate ions, whose concentrations are typically low, can exhibit sharp increases under specific atmospheric conditions, such as intense precipitation events or NPF episodes (Tammiet et al., 2014; Leino et al., 2016). For this reason, intermediate ions are valuable for identifying and characterising NPF events.

70 Recently, Kulmala et al. (2022) suggested that the NPF mechanism should be considered differently and NPF can occur even on days that are usually considered non-event days, such events are termed “quiet” NPF (QNPF) events. They also developed a methodology to actually detect and quantify the intensity of QNPF. To date, QNPF events have been reported and investigated in boreal forests and urban sites in central Europe (Kulmala et al., 2022), as well as in a megacity in eastern China (Zhang et al., 2025) and in the Amazon boundary layer (Meller et al., 2025). These episodes contribute significantly to the

75 number concentrations of nucleation-mode particles. Furthermore, the dynamic properties (i.e., formation and growth rate) of the freshly formed particles are relatively similar between a typical NPF and QNPF day (Kulmala et al., 2022). This finding fundamentally changes the way in which we classify and analyze NPF dynamics, leading to a radical transformation in NPF studies (Kulmala et al., 2024). Within this framework, Aliaga et al. (2023) introduced a new probabilistic tool for evaluating the occurrence and intensity of NPF events, called the nanoparticle ranking analysis method.

80 This study applies this newly proposed method to gain fresh insights into NPF events in the marine background of the eastern Mediterranean. We examine the role of ions in identifying and classifying NPF events using three years of measurements of ion and neutral PNSD at Finokalia in Crete, Greece.

2 Materials and Methods

2.1 Site description

85 Ion and PNSD were measured at the Finokalia environmental research station of the University of Crete (<https://finokalia.chemistry.uoc.gr>) during a three-year period, from June 2020 to May 2023. Finokalia station is a European super-site for aerosol research, part of the ACTRIS Network (<https://www.actris.eu/>). The station is located on the north-eastern part of Crete (35° 24' N, 25° 60', 250 a.s.l.), facing the sea in the broad north sector, situated on a hill above the coastline. Finokalia is representative of the background marine conditions of eastern Mediterranean (Kouvarakis et al., 2002; 90 Lelieveld et al., 2002), with no significant human activity within 15 km. The nearest city is Heraklion with almost 180,000 inhabitants, located 50 km west of Finokalia.

2.2 Measurements

Ion number size distributions were measured using a Neutral cluster and Air Ion Spectrometer (NAIS; Manninen et al., 2016; Mirme and Mirme, 2013), providing mobility distributions of air ions (0.8–42 nm) and total particles (2–42 nm) across 28 size-



95 ranges. A full measurement circle was performed every 5 min (2 min ions, 2 min particles, 1 min offset). The NAIS inlet tube had a diameter of 35 mm with a sample flow rate of 60 L min⁻¹. Diffusional losses within the inlet tubing were considered negligible; however, losses in the sampling lines were accounted for during data inversion. The NAIS system underwent a calibration workshop in 2025 at the Cluster Calibration Center (CCC) which is hosted by Institute for Atmospheric and Earth System Research (INAR), University of Helsinki, Finland (<https://www.actris-ecac.eu/ccc.html#CCC>). In both particle and
100 ion modes, the sizing accuracy was within 20% of the reference DMA. For negative ions at 3 nm, the detection efficiency in the ion mode was less than 20% of the reference, although the positive mode differed from the reference by a reasonable amount. The detection efficiency for positive mode in particle mode ranged from 40% less than reference at 4 nm to around 30% more than reference at 10 nm. When compared to the reference instrument, the negative mode detection efficiency fell within an acceptable range. Additionally, PNSDs (9–850 nm) were measured every 5 min with a TROPOS type mobility
105 particle size spectrometer (MPSS) (Kalivitis et al., 2019). PNSD data covered only 200 common days with NAIS due to MPSS malfunctions.

Radon activity concentrations were determined by active deposition onto a 13.8 cm² moving cellulose filter and detection of short-lived progeny (²¹⁸Po, ²¹⁴Po) using an LSCE moving-filter progeny monitor, with 2 h ambient air sampling at 12–14 m³ h⁻¹ (deposition velocity ~1 m s⁻¹) (Schmithüsen et al., 2017).

110 Meteorological parameters, including wind speed and direction, temperature, relative humidity and solar radiation, were continuously monitored throughout the study period by an automatic weather station installed at an altitude of 2 m at Finokalia. The time resolution for all measurements was 5 minutes.

2.3 Event based NPF classification

Based on an extensively approach proposed by Dal Maso et al. (2005), measurement days were classified into “NPF”, “non-
115 NPF”, and “undefined” using the daily distributions from NAIS. A day can be classified as “NPF” when: i) a new nucleation-mode distinctly appears, ii) this new mode persists for at least 1 h, and iii) it shows signs of gradual growth, exhibiting a characteristic “banana-shaped” pattern. This study used negative polarity due to its better representation of NPF (Kalivitis et al., 2012). NPF events were further classified as i) Class I when the evolution of particle size and number concentration could be clearly observed and the dynamic properties could be retrieved, and as ii) Class II when variations in the nucleation-mode
120 concentrations made it difficult or impossible to describe the event dynamics.

The formation rate (J_{dp} ; particles cm⁻³ s⁻¹) describes the net flux of changes in the number concentration of particles in the nucleation range, and can be calculated following the methodology by Kulmala et al. (2012). The growth rate of particles from d_i to d_j ($GR_{(d_i-d_j)}$; nm h⁻¹) is estimated from the slope of a first-order polynomial fit to the growing geometric mean diameter (GMD) of the nucleation-mode particles as a function of time (Dal Maso et al., 2005; Kulmala et al., 2012). For the present
125 analysis, only those events that are registered as Class I are used, as J_{dp} and $GR_{(d_i-d_j)}$ could be determined with high confidence according to Hirsikko et al. (2011). Condensation sink (CS; s⁻¹) shows how rapidly gaseous compounds condense on available



aerosol particle's surface (Kerminen et al., 2018), and is calculated following Kulmala et al. (2012). The coagulation sink (CoagS; s^{-1}) reflects the coagulation rate of particles above a certain diameter (d_p) and is determined using the approach proposed by Kerminen et al. (2001).

130 2.4 The ranking analysis method

The nanoparticle ranking analysis method proposed by Aliaga et al. (2023) was applied to focus on the smaller available nanoparticle measurement sizes and observe NPF phenomena on days classified as “non-event”. This method considers particle and ion concentrations in the 2.5 to 5 nm size range ($N_{2.5-5}$). The selected size limits are set to avoid interference from molecular clusters (low limit) and from any randomly occurring primary sources of ultrafine particles (upper limit) (Aliaga et al., 2023).

135 The methodology is outlined as follows. First, a median 2-hour rolling smoothing is performed to $N_{2.5-5}$. Then, “active” and “background” periods are identified based on the maximum and minimum diurnal concentrations of $N_{2.5-5}$, respectively. The background number concentration for each day is calculated as the median value of the smoothed $N_{2.5-5}$ during the background region, defined as the hours from night-time to early morning. The active peak number concentration is determined by the maximum value of $N_{2.5-5}$ during the active region in the daytime. The times of the two regions are obviously season dependent and are presented in Table 1. The $\Delta N_{2.5-5}$ value is then calculated as the difference between the active peak daytime number concentration and the background number concentration for each day. The $\Delta N_{2.5-5}$ is used to rank and group days into percentiles in order to assess potential NPF patterns. The main advantage of this approach is that it provides a probability distribution for all days for which data are available (Kulmala et al., 2024). Furthermore, it can be used combined with clustering techniques to categorize days depending on the dynamics of each event (Aliaga et al., 2025).

145 **Table 1: Definition of the of the time interval in UTC that “active” and “background” regions occur per season at the Finokalia environmental conditions.**

TIME (UTC)	SUMMER	AUTUMN	WINTER	SPRING
Background region	01:00-07:00	01:00-08:30	01:00-08:00	01:00-05:00
Active region	07:00-16:00	08:30-15:30	09:00-18:00	06:30-15:00

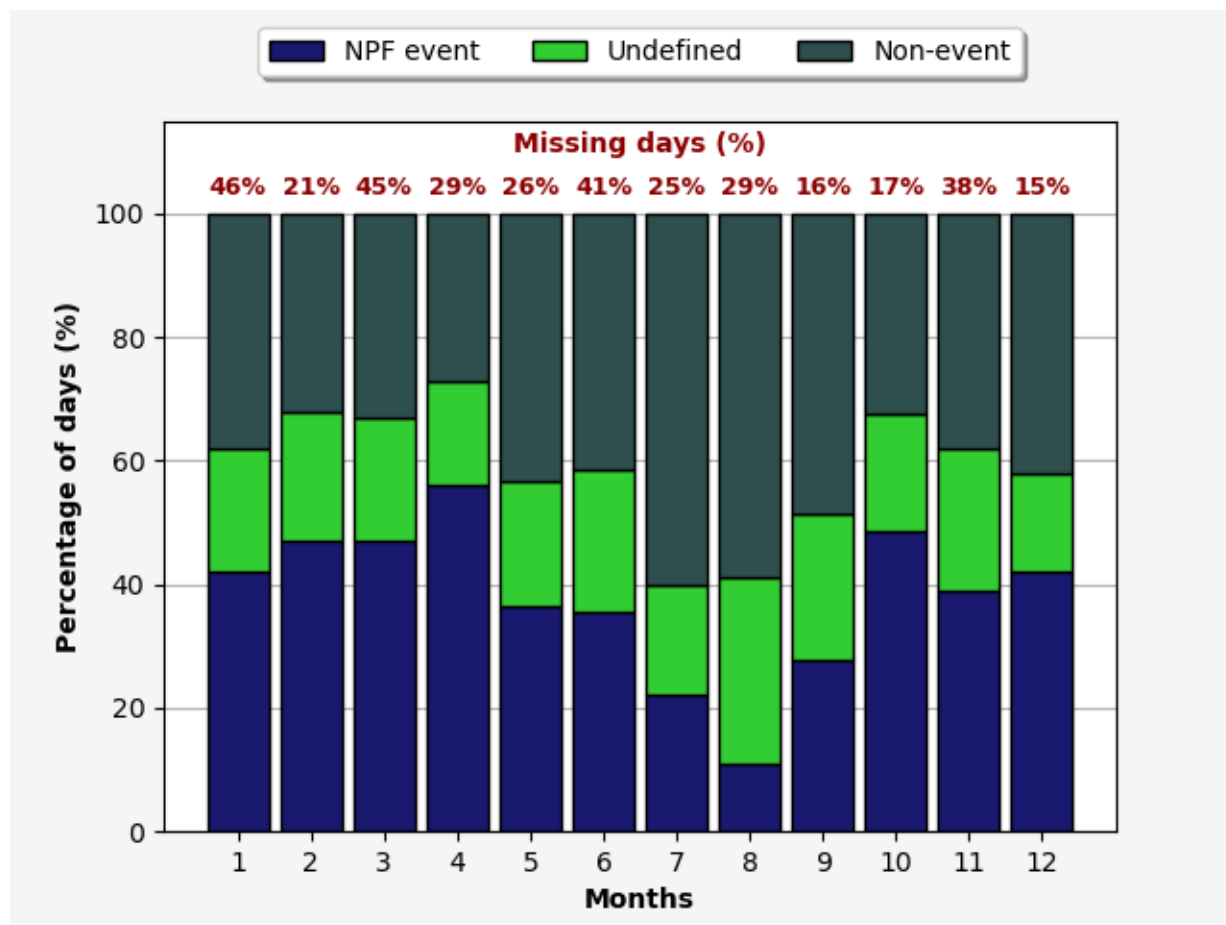
3 Results and discussion

3.1 Traditional classification of NPF

150 A total of 775 plots of daily ion and particle number size distributions (INSD) were analyzed. The relative frequency of the NPF events (Class I and II), as well as undefined and non-NPF event days, were determined following the methodology by Dal Maso et al. (2005) (section 2.3), is summarized in Fig.1 and Table 2. Over the three-year measurement period, the data coverage was 71% and all months presented coverage higher than 50%, indicating that the reported frequencies may be



considered representative (Fig. 1). The missing days were due to technical faults, maintenance issues or rain-affected
155 measurements, which usually occurred during winter. Of the valid observation days, 37% (n=291) were classified as NPF
event days, and 21% (n=162) were categorised as “undefined”. The annual average NPF frequency at Finokalia is somewhat
higher than the global NPF frequency range reported by Nieminen et al. (2018), where the median NPF frequency varies from
8% to 31%. It lies at the upper limit of the NPF frequencies calculated using long-term PNSD measurements in the eastern
Mediterranean (10 to 36%) (Kopanakis et al., 2013; Kalivitis et al., 2019; Kalkavouras et al., 2020; Baalbaki et al., 2021). This
160 average value is 1.5 times higher than that reported by Kalivitis et al. (2019), based on 10 years of PNSD measurements. One
possible explanation for this difference is that NAIS data may be more indicative of local NPF events involving limited particle
growth. Such events may not be apparent in MPSS data. Nevertheless, an earlier study at Finokalia based on one year of AIS
measurements found a NPF frequency of 23% (Manninen et al., 2010).



165

Figure 1: Relative frequency of the NPF (class I and II), undefined and non-NPF event days classified according to the traditional event-based method by Dal Maso et al. (2005). Percentage of missing days is also presented for each month.



Table 2: Classification of all measuring days to event (Class I and II), undefined and non-event days according to the criteria of Dal Maso et al. (2005).

170

Days classification	Number of days	Frequency (%)
<i>Total events</i>	291	37
Class I	104	13
Class II	187	24
175 Undefined	162	21
Non-event	322	42
Total days	775	

NPF generally occurs throughout the year; however, it exhibits a clear seasonal pattern, with higher frequencies in winter and spring and lower frequencies in summer (Fig. 1). The highest monthly frequency of NPF episodes was observed in April (56%) owing to the higher emissions of biogenic aerosol precursor compounds and intensive photochemistry. A secondary maximum is found in October (48%), probably due to the onset of the wet period and the decrease in CS. The lowest frequencies of NPF events occurred in July (22%) and August (11%), due to the dominance of Etesian winds in the central Aegean and the high CS associated with the long-range pollution transport from the Balkans, as well as central and eastern Europe (Kalkavouras et al., 2017). The seasonality of NPF frequency is consistent with that reported by Baalbaki et al. (2021) for the Agia Marina Xyliatos station in Cyprus. Kalivitis et al. (2019) using MPSS data, found a similar seasonality at the Finokalia station in earlier years; however, analysis based on ion spectrometer data showed that the maximum event frequency occurred in March, although data were available for only 1.5 years. In contrast, Pikridas et al. (2012) reported a different annual variation at the same location, with the highest NPF frequency occurring in February and the lowest in August.

190

3.2 Identification of site-specific indicators for NPF

At Finokalia, the median number concentration of small, intermediate and large negative (positive) ions was found to be 216 cm^{-3} (254 cm^{-3}), 7 cm^{-3} (3 cm^{-3}), and 38 cm^{-3} (25 cm^{-3}), respectively. As expected, the intermediate ion concentrations remain low throughout the period under study and can be used to identify NPF (Hirsikko et al., 2011). A major research question to be answered is “which sizes and polarity are optimal for identifying an NPF event”. For this purpose, we analysed the number concentrations of intermediate ions, focusing only on diameters between 1.87 and 2.88 nm (geometric mean diameter) for both polarities, corresponding to the lower measuring bins of the “intermediate ions” size range. In Fig. 2, average diurnal variability for all the available measurement days is presented. For the lowest diameter under consideration (1.87 nm), positive ions have 68% higher concentrations than the negative ions and present clear daily variability with a mid-day increase, whereas negative

195



ions are more abundant at night. For the next size (2.16 nm), the concentrations of ions for both polarities decrease by factors between 2 and 10, reflecting the transition to the intermediate ion regime, which remains clearly unaffected by the small ion range. At this size, negative ions become 60% more abundant than positive ions. Diurnal variability also changes for the negative polarity, becoming more pronounced, with a sharp increase in concentrations around midday, which reflects an NPF event. For the remaining two diameter categories the daily patterns are similar to those at 2.16 nm, with the negative ions being relatively more abundant by 71% and 93% than the positive ones. Around noon, a ~50% enhancement in ion concentrations is observed, which can be attributed to NPF events. Therefore, it is reasonable to claim that the intermediate ion regime at Finokalia starts at a diameter of approximately 2 nm, and that slightly larger diameters may be used to identify and analyse events of intermediate ion formation.

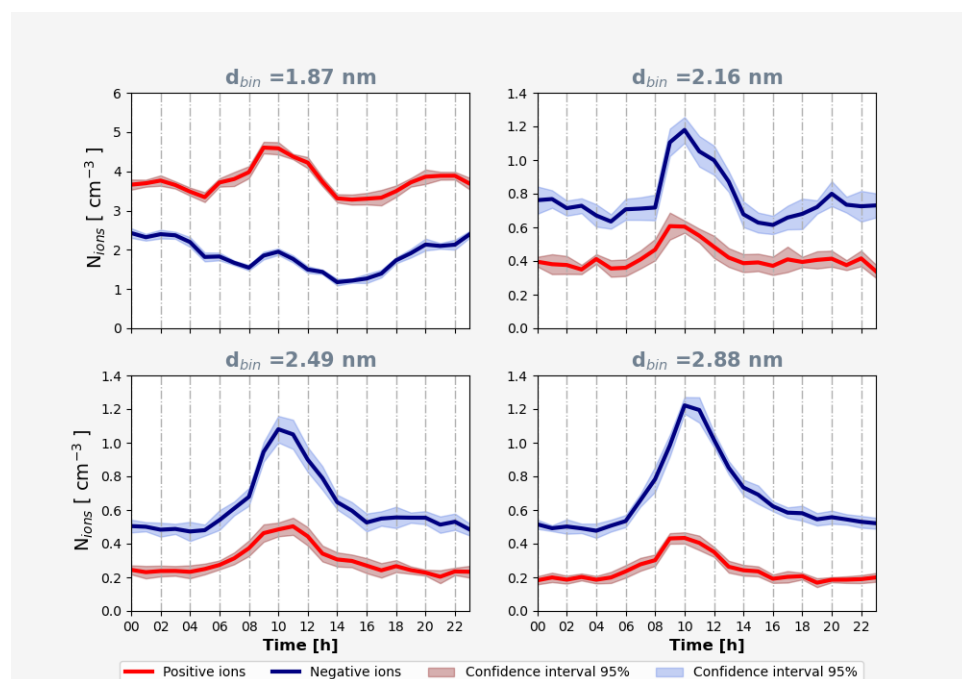


Figure 2: Average daily variation of ion concentrations for all available measurement days at the Finokalia station. Negative (blue) and positive (red) ion concentrations for diameters of 1.87, 2.16, 2.49 and 2.88 nm. The shaded area presents the 95% confidence intervals.

To choose the most suitable polarity for identifying these events, we investigated the relative standard deviation (RSD) of the intermediate ion concentrations (not shown). Higher RSD values were observed for negative polarity intermediate ions, indicating larger variability and more pronounced formation events. Thus, negative intermediate ions appear to be more suitable for detecting NPF episodes, in agreement with observations by Tuovinen et al. (2024) in a Finnish boreal environment. It should be noted that ion-based identification of NPF episodes may raise the question of sensitivity to ion-induced

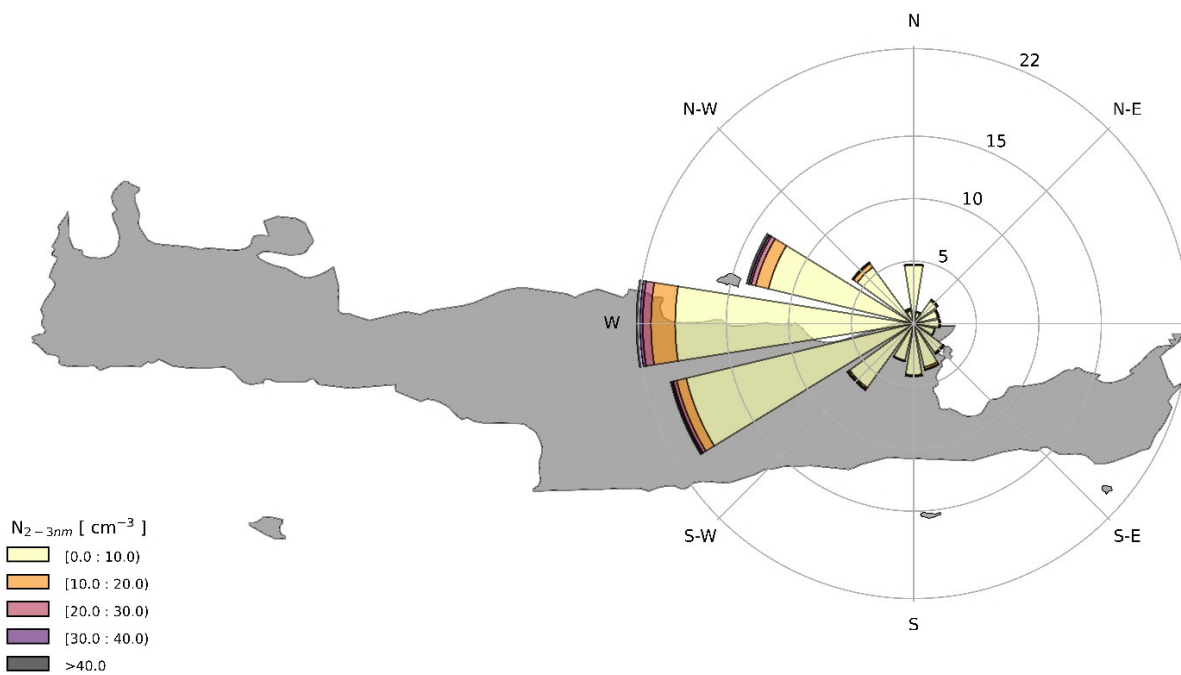


nucleation. However, owing to rapid charge–neutral equilibrium, intermediate ions mirror both charged and neutral particle
220 formation pathways (Leino et al., 2016) and can therefore be considered a proxy for total NPF activity.

A wind rose diagram was constructed using meteorological data and negative ion concentrations from the NAIS instrument in
the 2–3 nm size range to examine the relationship between the wind direction and ion concentrations (Fig. 3). The majority of
winds originated from the western and southern sectors, with 62% coming from the west, southwest, and south. In addition,
the west and southwest sectors contributed 58% to the total ion number concentrations. These results are consistent with
225 Kalkavouras et al. (2021) and Aktypis et al. (2024), who observed that during NPF events at the Finokalia station, air masses
mainly passed over the land in central Crete, possibly picking up ammonia and amine precursors essential for NPF activity.

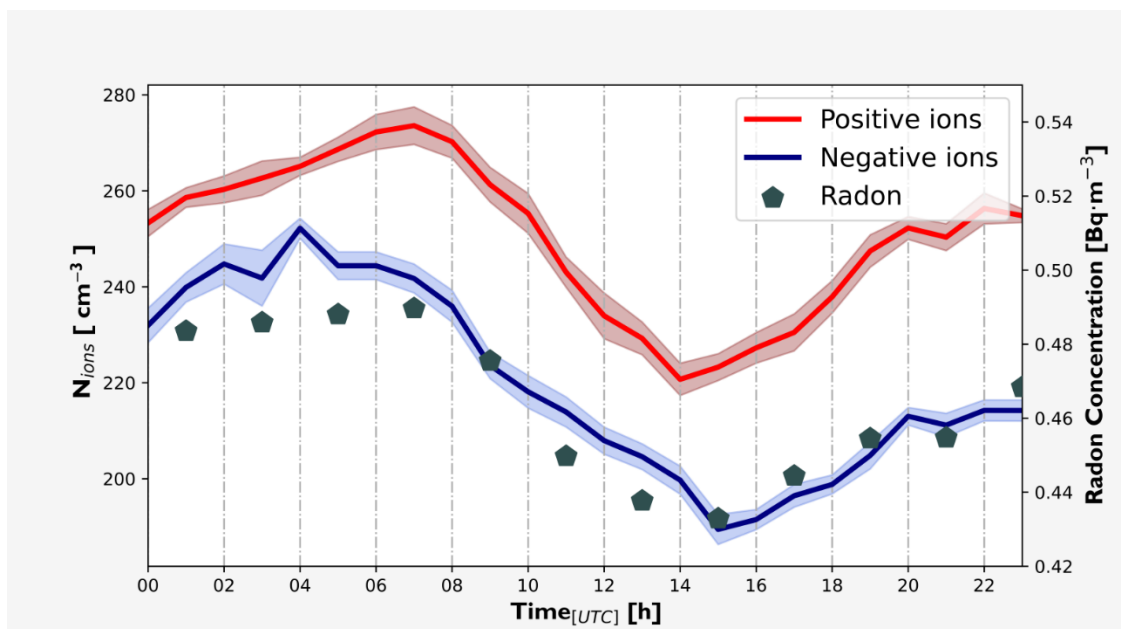
Radon decay has been suggested to contribute to NPF, since the emission of alpha particles during radioactive decay leads to
air molecule ionisation and may initiate ion-induced nucleation (Chen et al., 2016). Interestingly, the diurnal variation in radon
concentration measured at Finokalia correlates well with that of small ions (0.8 to 1.6 nm; Fig. 4). The average daily patterns
of both radon and small ions show a maximum between 03:00 and 07:00 UTC, followed by a minimum around 15:00 UTC,
230 which is consistent with boundary layer (BL) dynamics. During the night, the BL traps and accumulates radon near the surface
air layer, while during daytime, the enhanced BL promotes its dispersion. Locally produced small ions probably follow similar
dynamics, although further investigation is needed to quantify the contribution of radon decay to their production.

235



Figure

3: Wind rose diagram for ion concentrations at the Finokalia station on the island of Crete. The colour scale represents the concentration of negative ions in the 2-3 nm range.



255

Figure 4: Average diurnal cycle of atmospheric ion in the 0.8 to 1.6 nm size range and radon concentrations at the marine remote background environment of the Finokalia station.

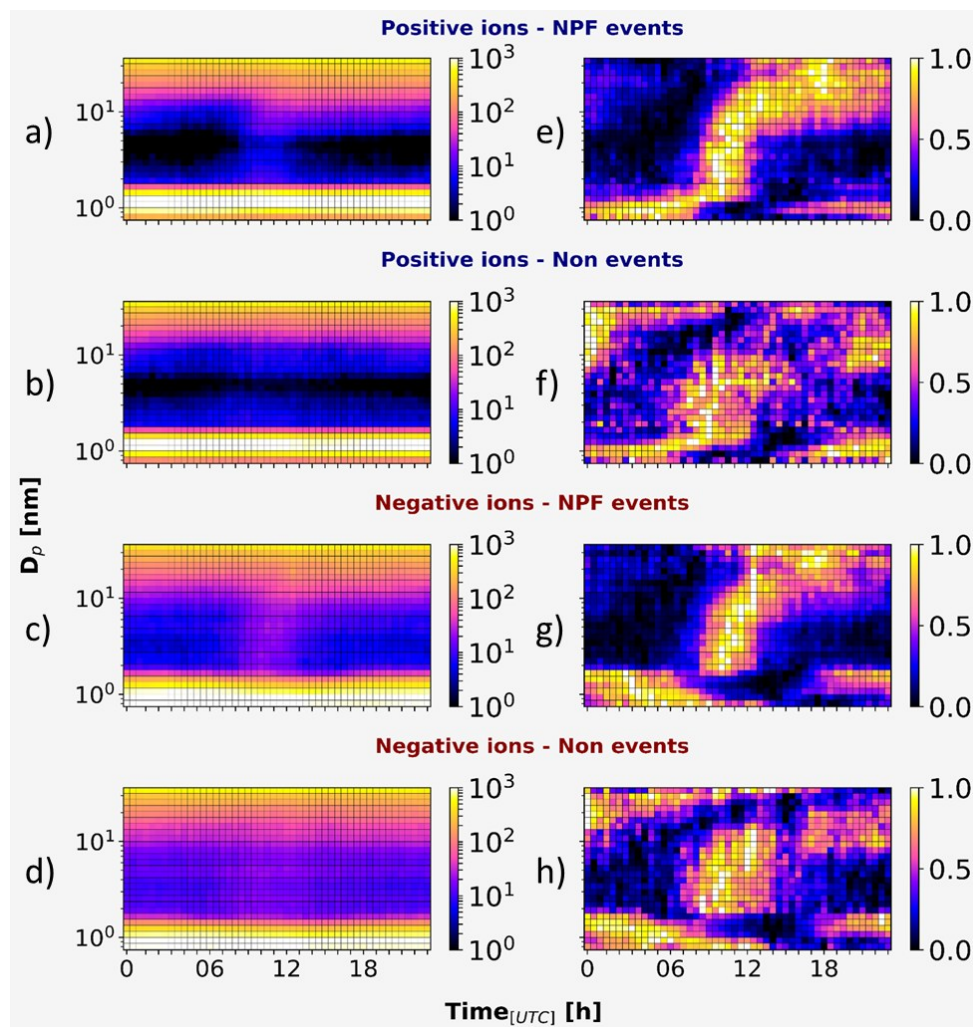
3.3 Quiet NPF in the Eastern Mediterranean

260 NPF appears to occur more frequently than suggested by traditional detection methods, particularly when analysis is performed on long-term averaged observations rather than daily variability. Although a long time series of MPSS data is available at Finokalia (Kalivitis et al., 2019), its lower cut-off size of 9 nm introduces uncertainties as to whether the detected NPF events come from local nucleation or reflect regional influences associated with transported particles. Observations from the NAIS instrument that measures ions and particles of diameters down to 0.8 nm, help fill this knowledge gap. Thus, we here focus on
265 the three years with available NAIS data that we analyse to detect QNPF at the Finokalia. As shown above, these measurements provide the necessary information on the sizes where NPF is actually taking place.

The NAIS data were classified as described in section 3.1. The undefined data were removed, and only the event and non-event days were analysed further, divided into two distinct groups (positive vs. negative). The ion number concentrations for each group on all days were averaged, and their average diurnal variations are presented in Fig. 5 (left column). For both
270 polarities on event days there is a growing mode at midday. On non-event days, there is some indication of intermediate ion formation around midday, particularly for negative polarity. Normalizing the average size distributions within each size bin with values ranging from 0 to 1 so that eventually only the shape of the size distribution matters, it becomes evident that both event and non-event days present intermediate ion formation and subsequent growth (Fig. 5, right column). A small difference in average growth rates is observed, with values of 1.2 and 2.6 nm h⁻¹ for positive ions and 2.2 and 3.7 nm h⁻¹ for negative ions



275 on non-event and event days, respectively. This relatively small difference in growth rates has also been reported for QNPF
events in different environments, such as a boreal forest in Finland and an urban site in Hungary (Kulmala et al., 2022).
Formation rates in the 3-7 nm size range (J_{3-7}) were 170% and 172% higher for negative than positive ions during NPF and
QNPF days, respectively. Remarkably, the average J_{3-7} for negative ions was 27% higher during QNPF compared to NPF
periods. For larger diameters (7-25 nm), J_{7-25} was 26% higher during NPF days; however, in both cases, it is clear the QNPF
280 contributed to the overall production of intermediate ions at Finokalia.
Daily production rates for 3-7 nm negative ions reached $449 \text{ cm}^{-3} \text{ day}^{-1}$ during QNPF days, compared to $341 \text{ cm}^{-3} \text{ day}^{-1}$ during
the common NPF periods. This indicates a constant production of intermediate ions, even when traditional classification does
not identify NPF events (Table 3). It is noteworthy that the production of positive ions in this size range is less than 10% of
that of negative ions (Table 3). For the 7-25 nm size range, negative ion production remains higher than that of positive ions,
285 with values of 1,812 and $1,391 \text{ cm}^{-3} \text{ day}^{-1}$ during NPF and QNPF periods, respectively. Considering that about 10% more non-
event than event days were observed (Table 2), the overall production of new particles at Finokalia is about comparable when
NPF and QNPF phenomena occur.



290 **Figure 5:** Average diurnal variation of ion number size distributions ($dN/d\log D_p$) for NPF event days (a) and (c), and non-event
 days (b) and (d), for positive and negative polarity respectively. Annual diurnal variation of concentrations normalized (from 0 to
 295 1) using the maximum concentration per channel for the same data e), f) and g), h) respectively. In the normalized distributions NPF
 is visible in all cases.

Table 3: Daily production estimation of atmospheric ions for the 3-7 and 7-25 nm range during NPF and QNPF periods (traditionally
 295 classified as event and non-event days respectively) in $\text{cm}^{-3} \text{day}^{-1}$.

3-7 nm	NPF	QNPF
Positive ions	27	33
Negative ions	341	449
7-25 nm		
Positive ions	932	687
Negative ions	1,812	1,391

300



3.4 Ranking analysis method to the NAIS dataset

As NPF occurs continuously and only its daily intensity varies, a new approach is used to characterize the examined days, involving the ion number size distributions. We further apply the “nanoparticle ranking analysis method” (Aliaga et al., 2023) to characterize the NPF phenomena at Finokalia (see section 2.4). The 2.5-5 nm size range used in this method is suitable for the Finokalia site, as it is largely unaffected by variations in cluster ion sizes and effectively reflects local formation of intermediate ions. The analysis is based on INSD data, focusing on negative ions measured by the NAIS. From the $\Delta N_{2.5-5}$ values calculated for all available measurement days, we assigned a rank to each day and grouped them into 5% intervals. Afterwards, the number size distributions in each interval were averaged (Fig.6).

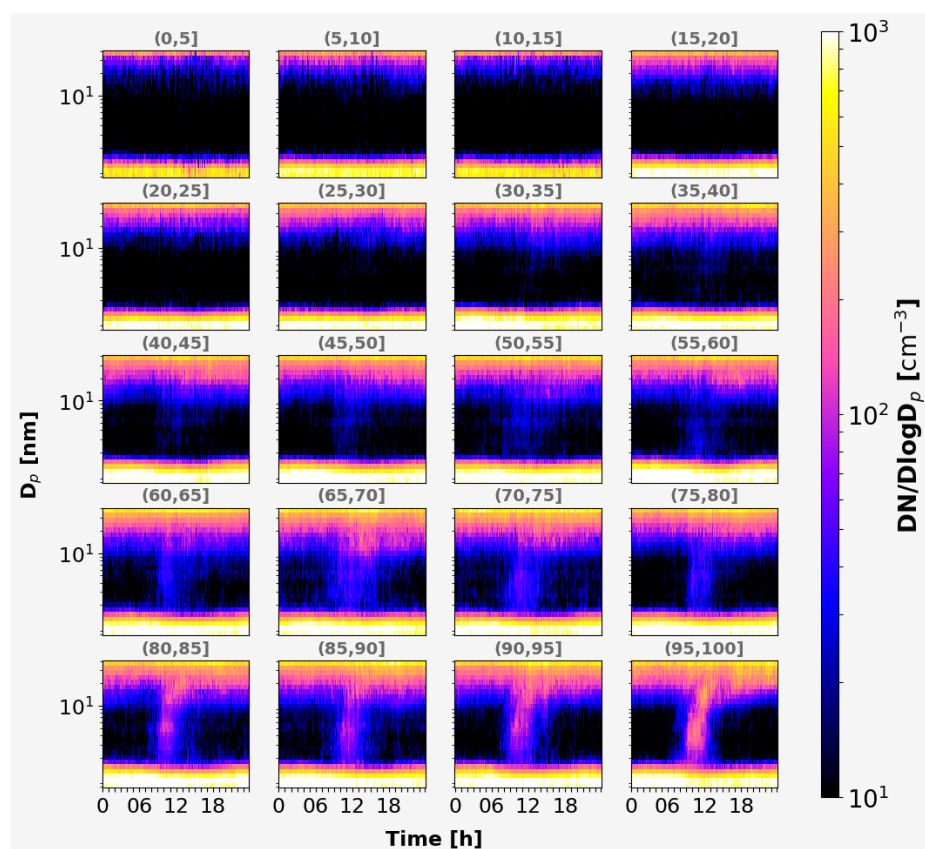


Figure 6: Daily ion number size distributions for the negative polarity ions from NAIS, grouped in 5% intervals based on the $\Delta N_{2.5-5}$ ranks in $dN/d\log D_p$ for all available measuring days.



320

Initial signs of NPF appear in the 40–45% range and become more pronounced from the 50–55% range onwards, providing a clear indication of an increase in charged particle concentrations. When applying the same normalization procedure as in section 3.3, the midday formation becomes noticeable even in the 25–30% interval (Fig.7). Therefore, intermediate ion formation is identified on at least 75% of the available days, twice as much compared to using the event-based NPF classification.

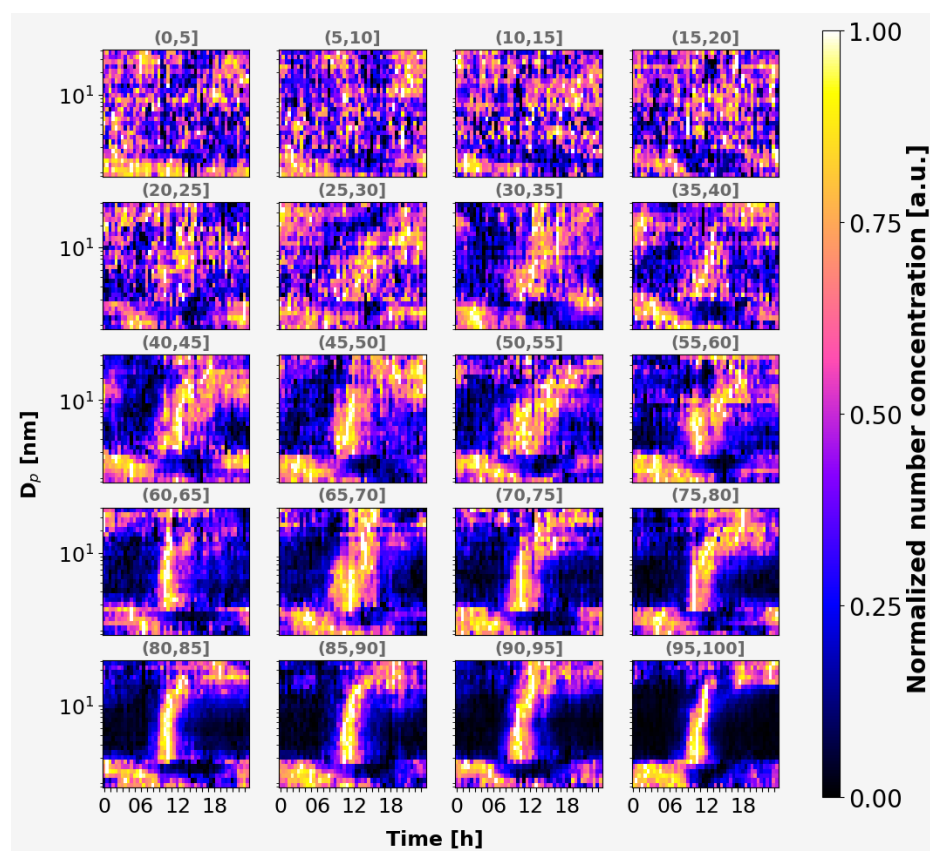


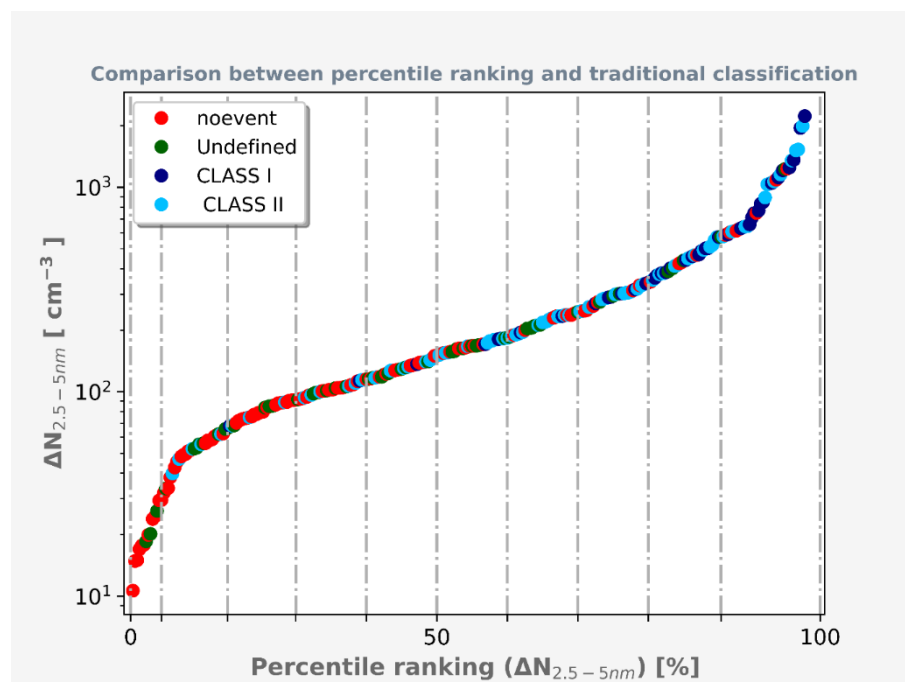
Figure 7: Normalised daily ion number size distributions for the negative polarity from NAIS grouped in 5% intervals based on the $\Delta N_{2.5-5}$ ranks and normalized to the maximum concentration for all available measuring days.

325

When these results are compared with the traditional classification scheme, it can be seen that the 35–40% interval is where more days start to be classified as event days (Fig.8). Overall, when using $\Delta N_{2.5-5}$ as the sole criterion, a clear escalation in



NPF intensity can be seen in the average plot for each interval.



330 **Figure 8:** Comparing the results of the ranking method to the traditional classification scheme using the $\Delta N_{2.5-5}$ metric and the subsequent percentile ranking in X and Y scales respectively.

The GR for intervals higher than 40-45% was calculated, and an increasing tendency was identified. For intervals below 70-75%, the GR was $2.5 \pm 1.1 \text{ nm h}^{-1}$, while for higher intervals the GR was $3.7 \pm 1.0 \text{ nm h}^{-1}$.

335 To assess how well particle production is captured, we examine the above classification in relation to the actual rate of particle formation. This analysis is limited by the availability of MPSS data needed to calculate the coagulation sink (CoagS), and hence the J_{3-7} and, therefore, was only possible for 200 days, where J_{3-7} was greater than $0.1 \text{ cm}^{-3} \text{ s}^{-1}$. As the values of $\Delta N_{2.5-5}$ increase, so do the rank and J_{3-7} , proving that the $\Delta N_{2.5-5}$ metric is indeed adequate for characterizing the intensity of the new particle formation (Fig. 9). As expected in all automated methods, there are days that would not traditionally be characterized as NPF days which fall within the upper percentile range. However, there is a clear tendency for Class I events to be correctly classified.

340

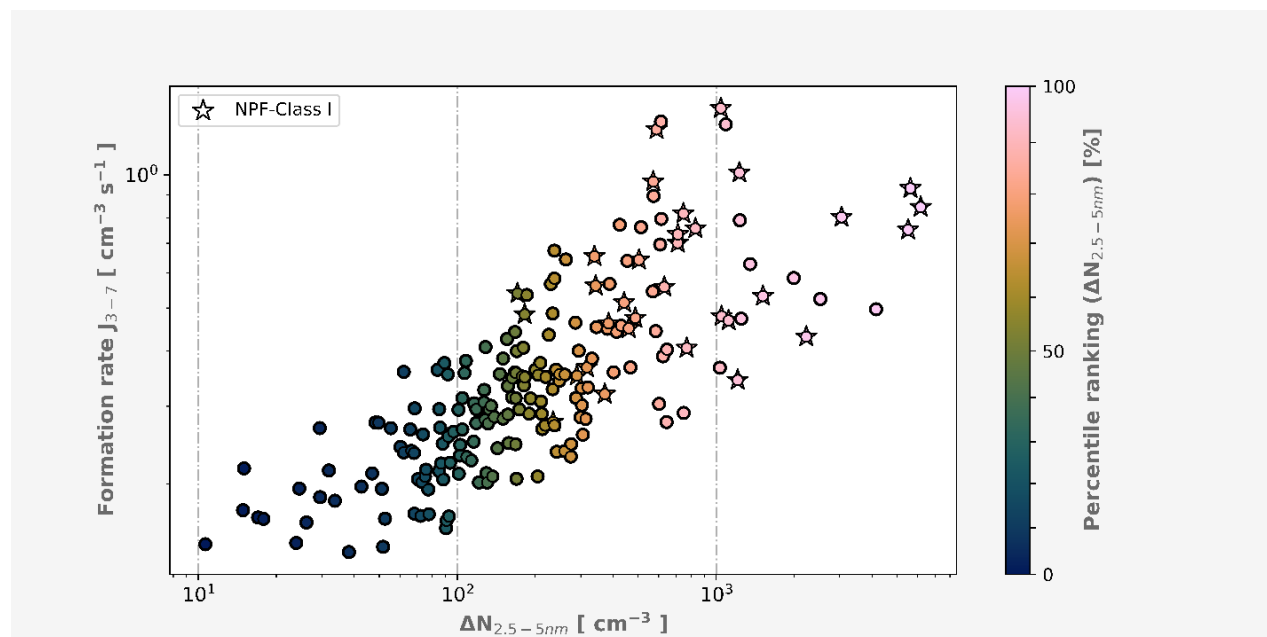


Figure 9: Daily formation rates of particles at negative polarity versus $\Delta N_{2.5-5}$. The color scale represents the percentile ranking, and stars indicate days traditionally classified as Class I NPF events.

345

4 Conclusions

Here, we present a fresh perspective on NPF at the remote marine environment of Finokalia, Greece, using ion and neutral particle concentration data and advanced analytical methodologies. Following the traditional event-based classification, NPF events were observed on approximately 37% of the examined days, exhibiting a notable seasonal pattern with higher frequencies in winter and spring. Intermediate ions show a pronounced increase in concentrations around midday and can be used as critical indicators of NPF events. Therefore, NPF events can be identified by the formation of ions that are larger than 2 nm. The study concludes that ions of negative polarity are a more reliable indicator for NPF events at the Finokalia station, as they present more pronounced formation events than positive ions. Our analysis indicates continuous particle formation even on days traditionally classified as “non-event” days, highlighting the need to reconsider the classification and analysis of NPF phenomena. When accounting for QNPF, the frequency of NPF events increases from 37 % to 75% of the observation days. QNPF events, although not traditionally classified as NPF days, show similar growth rates to common NPF events and contribute significantly to the nucleation-mode particle number concentrations. These results suggest the need for a fundamental change in how NPF events are classified and analysed, emphasizing the continuous nature of particle formation and the significant impact of QNPF events on regional and global aerosol dynamics.

360



Code availability

Software used to process and visualize the data are available at Zenodo via Kalivitis, N. (2025)
365 <https://doi.org/10.5281/zenodo.13771637>. For the NAIS data analysis the nais-processor code project was used, available at
Zenodo via jlpl. (2024) <https://doi.org/10.5281/zenodo.13819677>.

Data availability

Raw and processed data used in the study are openly available at Zenodo via Kalivitis, N. (2026)
<https://doi.org/10.5281/zenodo.19146913>.

370 Acknowledgements

We acknowledge support by Horizon Europe projects Net4Cities Contract No. 101138405 and Edu4ClimAte Contract No. 101071247, ACCC Flagship funded by the Academy of Finland grant number 337549 (UH) and 337552 (FMI), Academy professorship funded by the Academy of Finland (grant no. 302958), Academy of Finland projects no. 1325656, 311932, 334792, 316114, 325647, 325681, 347782, “Quantifying carbon sink, CarbonSink+ and their interaction with air quality”
375 INAR project funded by Jane and Aatos Erkkö Foundation, “Gigacity” project funded by Wihuri foundation, European Research Council (ERC) project ATM-GTP Contract No. 742206. The authors would like to thank Victor Kazan and Clément Narbaud for maintaining these measurements.

References

Aktypis, A., Kaltsonoudis, C., Patoulias, D., Kalkavouras, P., Matrali, A., Vasilakopoulou, C. N., Kostenidou, E., Florou, K.,
380 Kalivitis, N., Bougiatioti, A., Eleftheriadis, K., Vratolis, S., Gini, M. I., Kouras, A., Samara, C., Lazaridis, M., Chatoutsidou, S.-E., Mihalopoulos, N., and Pandis, S. N.: Significant spatial gradients in new particle formation frequency in Greece during summer, *Atmospheric Chemistry and Physics*, 24, 65–84, <https://doi.org/10.5194/acp-24-65-2024>, 2024.

Aliaga, D., Tuovinen, S., Zhang, T., Lampilahti, J., Li, X., Ahonen, L., Kokkonen, T., Nieminen, T., Hakala, S., Paasonen, P.,
385 Bianchi, F., Worsnop, D., Kerminen, V.-M., and Kulmala, M.: Nanoparticle ranking analysis: determining new particle



- formation (NPF) event occurrence and intensity based on the concentration spectrum of formed (sub-5 nm) particles, *Aerosol Research*, 1, 81–92, <https://doi.org/10.5194/ar-1-81-2023>, 2023.
- Aliaga, D., Sinclair, V. A., Krejci, R., Andrade, M., Artaxo, P., Blacutt, L., Cai, R., Carbone, S., Gramlich, Y., Heikkinen, L., Heslin-Rees, D., Huang, W., Kerminen, V.-M., Koenig, A. M., Kulmala, M., Laj, P., Mardoñez-Balderrama, V., Mohr, C.,
390 Moreno, I., Paasonen, P., Scholz, W., Sellegri, K., Ticona, L., Uzu, G., Velarde, F., Wiedensohler, A., Worsnop, D., Wu, C., Xuemeng, C., Zha, Q., and Bianchi, F.: New particle formation dynamics in the central Andes: contrasting urban and mountaintop environments, *Aerosol Research*, 3, 15–44, <https://doi.org/10.5194/ar-3-15-2025>, 2025.
- Baalbaki, R., Pikridas, M., Jokinen, T., Laurila, T., Dada, L., Bezantakos, S., Ahonen, L., Neitola, K., Maisser, A., Bimenyimana, E., Christodoulou, A., Unga, F., Savvides, C., Lehtipalo, K., Kangasluoma, J., Biskos, G., Petäjä, T., Kerminen,
395 V.-M., Sciare, J., and Kulmala, M.: Towards understanding the characteristics of new particle formation in the Eastern Mediterranean, *Atmospheric Chemistry and Physics*, 21, 9223–9251, <https://doi.org/10.5194/acp-21-9223-2021>, 2021.
- Buenrostro Mazon, S., Riipinen, I., Schultz, D. M., Valtanen, M., Dal Maso, M., Sogacheva, L., Junninen, H., Nieminen, T., Kerminen, V.-M., and Kulmala, M.: Classifying previously undefined days from eleven years of aerosol-particle-size distribution data from the SMEAR II station, Hyytiälä, Finland, *Atmospheric Chemistry and Physics*, 9, 667–676,
400 <https://doi.org/10.5194/acp-9-667-2009>, 2009.
- Chen, X., Kerminen, V.-M., Paatero, J., Paasonen, P., Manninen, H. E., Nieminen, T., Petäjä, T., and Kulmala, M.: How do air ions reflect variations in ionising radiation in the lower atmosphere in a boreal forest, *Atmospheric Chemistry and Physics*, 16, 14297–14315, <https://doi.org/10.5194/acp-16-14297-2016>, 2016.
- Dal Maso, M., Kulmala, M., Riipinen, I., Wagner, R., Hussein, T., Aalto, P. P., and Lehtinen, K. E. J.: Formation and growth
405 of fresh atmospheric aerosols: eight years of aerosol size distribution data from SMEAR II, Hyytiälä, Finland, *Boreal Environment Research*, 10, 323–336, 2005.
- Hirsikko, A., Nieminen, T., Gagné, S., Lehtipalo, K., Manninen, H. E., Ehn, M., Hörrak, U., Kerminen, V.-M., Laakso, L., McMurry, P. H., Mirme, A., Mirme, S., Petäjä, T., Tammet, H., Vakkari, V., Vana, M., and Kulmala, M.: Atmospheric ions and nucleation: a review of observations, *Atmospheric Chemistry and Physics*, 11, 767–798, <https://doi.org/10.5194/acp-11-767-2011>, 2011.
410
- jlpl: nais processor, , <https://doi.org/10.5281/zenodo.13819677>, 2024.
- Kalivitis, N., Birmili, W., Stock, M., Wehner, B., Massling, A., Wiedensohler, A., Gerasopoulos, E., and Mihalopoulos, N.: Particle size distributions in the Eastern Mediterranean troposphere, *Atmospheric Chemistry and Physics*, 8, 6729–6738, <https://doi.org/10.5194/acp-8-6729-2008>, 2008.
- 415 Kalivitis, N., Stavroulas, I., Bougiatioti, A., Kouvarakis, G., Gagné, S., Manninen, H. E., Kulmala, M., and Mihalopoulos, N.: Night-time enhanced atmospheric ion concentrations in the marine boundary layer, *Atmospheric Chemistry and Physics*, 12, 3627–3638, <https://doi.org/10.5194/acp-12-3627-2012>, 2012.
- Kalivitis, N., Kerminen, V.-M., Kouvarakis, G., Stavroulas, I., Tzitzikalaki, E., Kalkavouras, P., Daskalakis, N., Myriokefalitakis, S., Bougiatioti, A., Manninen, H. E., Roldin, P., Petäjä, T., Boy, M., Kulmala, M., Kanakidou, M., and



- 420 Mihalopoulos, N.: Formation and growth of atmospheric nanoparticles in the eastern Mediterranean: results from long-term measurements and process simulations, *Atmospheric Chemistry and Physics*, 19, 2671–2686, <https://doi.org/10.5194/acp-19-2671-2019>, 2019.
- Kalivitis, N.: Continuous new particle formation in a Mediterranean coastal environment: Insights from atmospheric ions behaviour analysis, <https://doi.org/10.5281/zenodo.13771637>, 2025.
- 425 Kalivitis, N.: Continuous new particle formation in a Mediterranean coastal environment: Insights from atmospheric ions behaviour analysis, <https://doi.org/10.5281/zenodo.19146913>, 2026.
- Kalkavouras, P., Bossioli, E., Bezantakos, S., Bougiatioti, A., Kalivitis, N., Stavroulas, I., Kouvarakis, G., Protonotariou, A. P., Dandou, A., Biskos, G., Mihalopoulos, N., Nenes, A., and Tombrou, M.: New particle formation in the southern Aegean Sea during the Etesians: importance for CCN production and cloud droplet number, *Atmospheric Chemistry and Physics*, 17,
- 430 175–192, <https://doi.org/10.5194/acp-17-175-2017>, 2017.
- Kalkavouras, P., Bougiatioti, A., Grivas, G., Stavroulas, I., Kalivitis, N., Liakakou, E., Gerasopoulos, E., Pilinis, C., and Mihalopoulos, N.: On the regional aspects of new particle formation in the Eastern Mediterranean: A comparative study between a background and an urban site based on long term observations, *Atmospheric Research*, 239, 104911, <https://doi.org/10.1016/j.atmosres.2020.104911>, 2020.
- 435 Kalkavouras, P., Bougiatioti, A., Hussein, T., Kalivitis, N., Stavroulas, I., Michalopoulos, P., and Mihalopoulos, N.: Regional New Particle Formation over the Eastern Mediterranean and Middle East, *Atmosphere*, 12, 13, <https://doi.org/10.3390/atmos12010013>, 2021.
- Kerminen, V.-M., Pirjola, L., and Kulmala, M.: How significantly does coagulation limit atmospheric particle production?, *Journal of Geophysical Research: Atmospheres*, 106, 24119–24125, <https://doi.org/10.1029/2001JD000322>,
- 440 2001.
- Kerminen, V.-M., Chen, X., Vakkari, V., Petäjä, T., Kulmala, M., and Bianchi, F.: Atmospheric new particle formation and growth: review of field observations, *Environ. Res. Lett.*, 13, 103003, <https://doi.org/10.1088/1748-9326/aadf3c>, 2018.
- Kopanakis, I., Chatoutsidou, S. E., Torseth, K., Glytsos, T., and Lazaridis, M.: Particle number size distribution in the eastern Mediterranean: Formation and growth rates of ultrafine airborne atmospheric particles, *Atmospheric Environment*, 77, 790–
- 445 802, <https://doi.org/10.1016/j.atmosenv.2013.05.066>, 2013.
- Kouvarakis, G., Vrekoussis, M., Mihalopoulos, N., Kourtidis, K., Rappenglueck, B., Gerasopoulos, E., and Zerefos, C.: Spatial and temporal variability of tropospheric ozone (O₃) in the boundary layer above the Aegean Sea (eastern Mediterranean), *Journal of Geophysical Research: Atmospheres*, 107, PAU 4-1-PAU 4-14, <https://doi.org/10.1029/2000JD000081>, 2002.
- Kulmala, M., Petäjä, T., Nieminen, T., Sipilä, M., Manninen, H. E., Lehtipalo, K., Dal Maso, M., Aalto, P. P., Junninen, H.,
- 450 Paasonen, P., Riipinen, I., Lehtinen, K. E. J., Laaksonen, A., and Kerminen, V.-M.: Measurement of the nucleation of atmospheric aerosol particles, *Nat Protoc*, 7, 1651–1667, <https://doi.org/10.1038/nprot.2012.091>, 2012.
- Kulmala, M., Petäjä, T., Ehn, M., Thornton, J., Sipilä, M., Worsnop, D. R., and Kerminen, V.-M.: Chemistry of Atmospheric Nucleation: On the Recent Advances on Precursor Characterization and Atmospheric Cluster Composition in Connection with



- Atmospheric New Particle Formation, *Annual Review of Physical Chemistry*, 65, 21–37, <https://doi.org/10.1146/annurev-physchem-040412-110014>, 2014.
- 455 Kulmala, M., Kerminen, V.-M., Petäjä, T., Ding, A. J., and Wang, L.: Atmospheric gas-to-particle conversion: why NPF events are observed in megacities?, *Faraday Discuss.*, 200, 271–288, <https://doi.org/10.1039/C6FD00257A>, 2017.
- Kulmala, M., Junninen, H., Dada, L., Salma, I., Weidinger, T., Thén, W., Vörösmarty, M., Komsaare, K., Stolzenburg, D., Cai, R., Yan, C., Li, X., Deng, C., Jiang, J., Petäjä, T., Nieminen, T., and Kerminen, V.-M.: Quiet New Particle Formation in
460 the Atmosphere, *Front. Environ. Sci.*, 10, <https://doi.org/10.3389/fenvs.2022.912385>, 2022.
- Kulmala, M., Aliaga, D., Tuovinen, S., Cai, R., Junninen, H., Yan, C., Bianchi, F., Cheng, Y., Ding, A., Worsnop, D. R., Petäjä, T., Lehtipalo, K., Paasonen, P., and Kerminen, V.-M.: Opinion: A paradigm shift in investigating the general characteristics of atmospheric new particle formation using field observations, *Aerosol Research*, 2, 49–58, <https://doi.org/10.5194/ar-2-49-2024>, 2024.
- 465 Leino, K., Nieminen, T., Manninen, H. E., Petäjä, T., Kerminen, V.-M., and Kulmala, M.: Intermediate ions as a strong indicator of new particle formation bursts in a boreal forest, *Boreal Environment Research*, 21, 274–286, 2016.
- Lelieveld, J., Berresheim, H., Borrmann, S., Crutzen, P. J., Dentener, F. J., Fischer, H., Feichter, J., Flatau, P. J., Heland, J., Holzinger, R., Korrmann, R., Lawrence, M. G., Levin, Z., Markowicz, K. M., Mihalopoulos, N., Minikin, A., Ramanathan, V., de Reus, M., Roelofs, G. J., Scheeren, H. A., Sciare, J., Schlager, H., Schultz, M., Siegmund, P., Steil, B., Stephanou, E.
470 G., Stier, P., Traub, M., Warneke, C., Williams, J., and Ziereis, H.: Global Air Pollution Crossroads over the Mediterranean, *Science*, 298, 794–799, <https://doi.org/10.1126/science.1075457>, 2002.
- Manninen, H. E., Nieminen, T., Asmi, E., Gagné, S., Häkkinen, S., Lehtipalo, K., Aalto, P., Vana, M., Mirme, A., Mirme, S., Hörrak, U., Plass-Dülmer, C., Stange, G., Kiss, G., Hoffer, A., Törö, N., Moerman, M., Henzing, B., de Leeuw, G., Brinkenberg, M., Kouvarakis, G. N., Bougiatioti, A., Mihalopoulos, N., O’Dowd, C., Ceburnis, D., Arneth, A., Svenningsson,
475 B., Swietlicki, E., Tarozzi, L., Decesari, S., Facchini, M. C., Birmili, W., Sonntag, A., Wiedensohler, A., Boulon, J., Sellegri, K., Laj, P., Gysel, M., Bukowiecki, N., Weingartner, E., Wehrle, G., Laaksonen, A., Hamed, A., Joutsensaari, J., Petäjä, T., Kerminen, V.-M., and Kulmala, M.: EUCAARI ion spectrometer measurements at 12 European sites – analysis of new particle formation events, *Atmospheric Chemistry and Physics*, 10, 7907–7927, <https://doi.org/10.5194/acp-10-7907-2010>, 2010.
- Manninen, H. E., Mirme, S., Mirme, A., Petäjä, T., and Kulmala, M.: How to reliably detect molecular clusters and nucleation
480 mode particles with Neutral cluster and Air Ion Spectrometer (NAIS), *Atmospheric Measurement Techniques*, 9, 3577–3605, <https://doi.org/10.5194/amt-9-3577-2016>, 2016.
- Meller, B. B., Franco, M. A., Valiati, R., Pöhlker, C., Machado, L. A. T., Ditas, F., Krempner, L. A., Raj, S. S., Dias-Júnior, C. Q., D’Oliveira, F. A. F., Rizzo, L. V., Pöschl, U., and Artaxo, P.: Quiet New Particle Formation is a significant aerosol source in the Amazon boundary layer, <https://doi.org/10.5194/egusphere-2025-4581>, 26 September 2025.
- 485 Merikanto, J., Spracklen, D. V., Mann, G. W., Pickering, S. J., and Carslaw, K. S.: Impact of nucleation on global CCN, *Atmospheric Chemistry and Physics*, 9, 8601–8616, <https://doi.org/10.5194/acp-9-8601-2009>, 2009.



- Mirme, S. and Mirme, A.: The mathematical principles and design of the NAIS – a spectrometer for the measurement of cluster ion and nanometer aerosol size distributions, *Atmospheric Measurement Techniques*, 6, 1061–1071, <https://doi.org/10.5194/amt-6-1061-2013>, 2013.
- 490 Nieminen, T., Kerminen, V.-M., Petäjä, T., Aalto, P. P., Arshinov, M., Asmi, E., Baltensperger, U., Beddows, D. C. S., Beukes, J. P., Collins, D., Ding, A., Harrison, R. M., Henzing, B., Hooda, R., Hu, M., Hörrak, U., Kivekäs, N., Komsaare, K., Krejci, R., Kristensson, A., Laakso, L., Laaksonen, A., Leitch, W. R., Lihavainen, H., Mihalopoulos, N., Németh, Z., Nie, W., O’Dowd, C., Salma, I., Sellegri, K., Svenningsson, B., Swietlicki, E., Tunved, P., Ulevicius, V., Vakkari, V., Vana, M., Wiedensohler, A., Wu, Z., Virtanen, A., and Kulmala, M.: Global analysis of continental boundary layer new particle formation
495 based on long-term measurements, *Atmospheric Chemistry and Physics*, 18, 14737–14756, <https://doi.org/10.5194/acp-18-14737-2018>, 2018.
- Pikridas, M., Riipinen, I., Hildebrandt, L., Kostenidou, E., Manninen, H., Mihalopoulos, N., Kalivitis, N., Burkhardt, J. F., Stohl, A., Kulmala, M., and Pandis, S. N.: New particle formation at a remote site in the eastern Mediterranean, *Journal of Geophysical Research: Atmospheres*, 117, <https://doi.org/10.1029/2012JD017570>, 2012.
- 500 Schmithüsen, D., Chambers, S., Fischer, B., Gilge, S., Hatakka, J., Kazan, V., Neubert, R., Paatero, J., Ramonet, M., Schlosser, C., Schmid, S., Vermeulen, A., and Levin, I.: A European-wide ²²²radon and ²²²radon progeny comparison study, *Atmospheric Measurement Techniques*, 10, 1299–1312, <https://doi.org/10.5194/amt-10-1299-2017>, 2017.
- Tammet, H., Komsaare, K., and Hörrak, U.: Intermediate ions in the atmosphere, *Atmospheric Research*, 135–136, 263–273, <https://doi.org/10.1016/j.atmosres.2012.09.009>, 2014.
- 505 Tuovinen, S., Lampilahti, J., Kerminen, V.-M., and Kulmala, M.: Intermediate ions as indicator for local new particle formation, *Aerosol Research*, 2, 93–105, <https://doi.org/10.5194/ar-2-93-2024>, 2024.
- Wang, J., Li, M., Li, L., Zheng, R., Fan, X., Hong, Y., Xu, L., Chen, J., and Hu, B.: Particle number size distribution and new particle formation in Xiamen, the coastal city of Southeast China in wintertime, *Science of The Total Environment*, 826, 154208, <https://doi.org/10.1016/j.scitotenv.2022.154208>, 2022.
- 510 Yan, C., Yin, R., Lu, Y., Dada, L., Yang, D., Fu, Y., Kontkanen, J., Deng, C., Garmash, O., Ruan, J., Baalbaki, R., Schervish, M., Cai, R., Bloss, M., Chan, T., Chen, T., Chen, Q., Chen, X., Chen, Y., Chu, B., Dällenbach, K., Foreback, B., He, X., Heikkinen, L., Jokinen, T., Junninen, H., Kangasluoma, J., Kokkonen, T., Kurppa, M., Lehtipalo, K., Li, H., Li, H., Li, X., Liu, Y., Ma, Q., Paasonen, P., Rantala, P., Pileci, R. E., Rusanen, A., Sarnela, N., Simonen, P., Wang, S., Wang, W., Wang, Y., Xue, M., Yang, G., Yao, L., Zhou, Y., Kujansuu, J., Petäjä, T., Nie, W., Ma, Y., Ge, M., He, H., Donahue, N. M., Worsnop,
515 D. R., Kerminen, V.-M., Wang, L., Liu, Y., Zheng, J., Kulmala, M., Jiang, J., and Bianchi, F.: The Synergistic Role of Sulfuric Acid, Bases, and Oxidized Organics Governing New-Particle Formation in Beijing, *Geophysical Research Letters*, 48, e2020GL091944, <https://doi.org/10.1029/2020GL091944>, 2021.
- Zhang, K., Feichter, J., Kazil, J., Wan, H., Zhuo, W., Griffiths, A. D., Sartorius, H., Zahorowski, W., Ramonet, M., Schmidt, M., Yver, C., Neubert, R. E. M., and Brunke, E.-G.: Radon activity in the lower troposphere and its impact on ionization rate:



- 520 a global estimate using different radon emissions, *Atmospheric Chemistry and Physics*, 11, 7817–7838,
<https://doi.org/10.5194/acp-11-7817-2011>, 2011.
- Zhang, R., Khalizov, A., Wang, L., Hu, M., and Xu, W.: Nucleation and Growth of Nanoparticles in the Atmosphere, *Chem. Rev.*, 112, 1957–2011, <https://doi.org/10.1021/cr2001756>, 2012.
- Zhang, T., Qi, X., Lampilahti, J., Chen, L., Chi, X., Nie, W., Huang, X., Zou, Z., Du, W., Kokkonen, T., Petäjä, T., Lehtipalo,
525 K., Kerminen, V.-M., Ding, A., and Kulmala, M.: Differential characterization of air ions in boreal forest of Finland and a
megacity of eastern China, *Atmospheric Chemistry and Physics*, 25, 10027–10048, [https://doi.org/10.5194/acp-25-10027-](https://doi.org/10.5194/acp-25-10027-2025)
2025, 2025.